Journal of Electronic Materials (2021) 50:5925–5932
https://doi.org/10.1007/s11664-021-09099-w

ORIGINAL RESEARCH ARTICLE

Metamaterial-Inspired Complementary Split Ring Resonator Sensor and Second-Order Approximation for Dielectric Characterization of Fluid

Anand Kumar[1] · Manvendra Singh Rajawat[2] · Santosh Kumar Mahto[3] · Rashmi Sinha[4]

Received: 6 October 2020 / Accepted: 30 June 2021 / Published online: 27 July 2021

Abstract

A metamaterial-based complementary split ring resonator (CSRR) structure is used to develop a sensor for dielectric characterization of fluids. The fluid present in the vertical column interacts with the fields around the CSRR causing a shift in the transmission coefficient curve (S_{21}). An empirical relationship can be established between the dielectric properties and the resonance frequency and Q-factor. This relationship is used for the dielectric characterization of the fluid. A second-order polynomial function is employed for a better curve fitting of the data to achieve higher accuracy in the prediction of complex permittivity (ε' and ε''). Multi-variate polynomial regression is used to determine the coefficients of the polynomial function. The proposed sensor predicts the permittivity of the sample with high accuracy. The design is very simple and the sample can be easily changed by replacing the glass tube. The sensor has very high sensitivity and requires a very little volume of the sample.

Keywords Metamaterial · Complementary split ring resonator (CSRR) · microwave sensor · dielectric characterization · permittivity · polynomial regression

Introduction

The application of microwave sensors in biomedical[1–5] and chemical[6–17] research areas has recently gained attention among researchers. Microwave sensors have hence found applications in food safety[18–21] and mechanical systems such as strain/displacement,[22–24] power[25,26] and pressure.[27] These sensors are inexpensive, robust, and offer high sensitivity.

Electromagnetic metamaterials are structures with engineered geometry and sub-wavelength resonators which can influence the electromagnetic waves. The metamaterials offer properties that do not exist or may not be easily accessible.[28] Split-ring resonators (SRR) or complementary split-ring resonators (CSRR) are popular because the use of SRRs/CSRRs reduces the patch size as it enables a shift in resonance frequency to a lower value.[29]

The SRRs and CSRRs have shown to have an electric field established around them, and changes in electrical properties of substances in the vicinity of the structure affect the resonance frequency and Q factor of the transmission coefficient curve of the sensor. In this paper, an empirical relationship is established between the relative permittivity and resonance frequency and Q factor, and the relationship is modeled by a second-order polynomial. Linear approximations of the relationship have been used in Refs. 7–10,13, which yields substantial error in predicting the permittivity. A multi-variate polynomial regression technique is used for solving the coefficients of the second-order polynomial.

The sensor is tested for two different solutions: methanol-water and ethanol-water. Ethanol (or ethyl alcohol) is an important industrial chemical and widely used as a solvent in the synthesis of other organic chemicals and as an additive to petrol. Methanol (or methyl alcohol) is used in manufacturing formaldehyde and other chemicals. The

✉ Anand Kumar
anandkumar13@iisc.ac.in

1 Dept. of Electrical Communication Engineering, Indian Institute of Science, Bengaluru 560012, India

2 Dept. of Mechanical Engineering, Indian Institute of Technology (ISM), Dhanbad 826004, India

3 Dept. of Electronics and Communication Engineering, Indian Institute of Information Technology, Ranchi 834010, India

4 Dept. of Electronics and Communication Engineering, National Institute of Technology, Jamshedpur 831014, India

proposed sensor finds its use in the industry as well as the laboratory.

The paper is divided into four sections. In Sect. "Sensor Design and Operation Principle", the design approach and the operation principle of the sensor device are discussed. In Sect. "Measurement and Analysis", the working of the sensor is discussed in detail using two different types of solutions: methanol-water in Sect. "Study of Methanol-Water Solution" and ethanol-water in Sect. "Study of Ethanol-Water Solution". A brief conclusion of the work presented in this paper is reported in Sect. "Conclusion", and the pseudo-code for multi-variate polynomial regression used in this paper is given in "Appendix A".

Sensor Design and Operation Principle

The structure comprises two concentric octagonal CSRR in the ground plane and a microstrip transmission line on the top. The overall size of the sensor is 25 mm × 20 mm. A substrate of 1.6 mm is chosen with relative permittivity 4.4 and dielectric loss tangent 0.02. A hole of diameter 1.5 mm is present in the center of the CSRR to place the glass capillary tube containing the sample fluid under investigation. The capillary tube is made replaceable so that samples can be replaced easily and avoids any error due to changes in concentration of the sample under test caused by the residue of the previous sample. Figure 1 shows the design of the proposed sensor along with the dimensions.

Figure 2 shows the distribution of the electric field around CSRR and in the capillary tube. The sample fluid inside the glass capillary influences the field distribution around the CSRR, which affects the transmission of the wave through the microstrip patch. Hence, the effects of change in the dielectric properties of fluid present in the glass capillary can be analyzed to establish a relationship with the transmission curve for the fluid.

The major part of the sensor is the CSRR which is etched on the ground plane. The CSRR is excited by the electric field coupled with the microstrip patch located on the upper surface. The coupled CSRR structure can be modeled by the lumped circuit shown in Fig. 3a.[29] In the equivalent circuit model, L and C_C model the inductance of the microstrip line, whereas the inductance, capacitance and resistance for CSRR is modeled by L_R, C_R and R_R, respectively.

The resonance frequency (f_o) observed as a notch in the transmission coefficient curve (S_{21}) can be found using Eq. 1 and the quality factor for the resonance can be calculated by Eq. 2.[30]

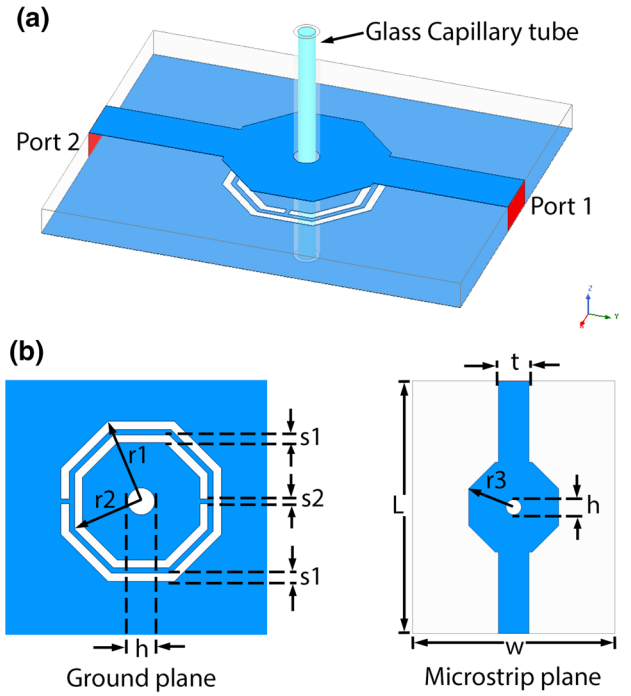

Fig. 1 (a) Proposed design of the sensor with glass capillary tube for holding sample fluid near CSRR, and (b) Structure of the octagonal CSRR and the transmission line with dimensions: $r1$ = 4.8 mm, $r2$ = 4 mm, $s1$ = 0.5 mm, $s2$ = 0.25 mm, h = 1.5 mm, $r3$ = 4.8 mm, t = 3 mm, L = 25 mm, w = 20 mm.

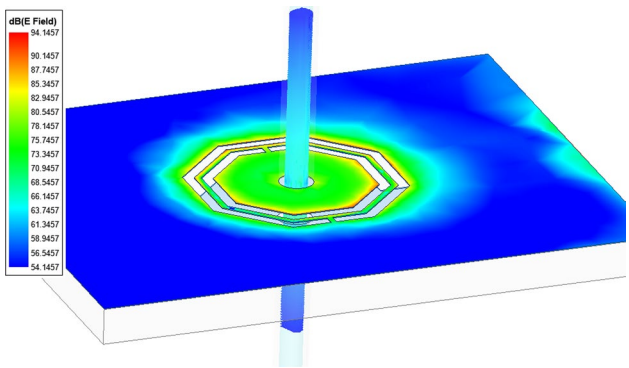

Fig. 2 Distribution of electric field around the CSRR and in the sample fluid (here methanol-water solution with 10% of water by volume).

$$f_o = \frac{1}{2\pi\sqrt{L_R(C_C + C_R)}} \tag{1}$$

$$Q = R\sqrt{\frac{C_C + C_R}{L_R}} \tag{2}$$

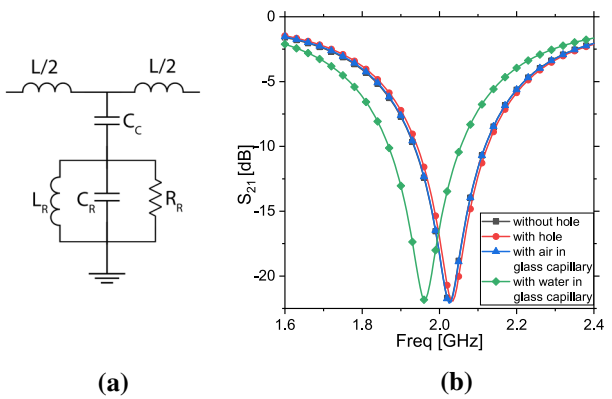

Fig. 3 (a) Equivalent circuit model of a CSRR, and (b) Effect of change in dielectric medium near the hole of CSRR on transmission coefficient (S_{21}).

The capacitance of CSRR is affected by the introduction of the capillary tube and the fluid sample. The effective capacitance of CSRR (C_R) can be thus expressed as a parallel combination of capacitance of dielectric substrate, glass capillary, and sample fluid given by Eq. 3.

$$C_R = C_o + C_{capillary} + C_{fluid} \tag{3}$$

Capacitance of a material is given by Eq. 4 where ε_o is the permittivity of free space, ε_{sample} is the relative permittivity of the dielectric material, A is the cross-sectional area and d thickness of the material.

$$C = \frac{\varepsilon_o \varepsilon_{sample} A}{d} \tag{4}$$

Now, since the permittivity is a complex quantity, it can be expressed as $\varepsilon_{sample} = \varepsilon' + j\varepsilon''$. From Eqs. 1–4, ε' and ε'' can be expressed as a function of resonance frequency (f_o) and Q factor (Q).

$$\begin{aligned} \varepsilon' &= f_1(f_o, Q), \\ \varepsilon'' &= f_2(f_o, Q) \end{aligned} \tag{5}$$

The transmission coefficient (S_{21}) curve for the structure proposed in Fig. 1 is plotted in Fig. 3b. Simulated results were generated by commercial high-frequency simulation software by ANSYS Electronics Desktop 2019R3. In the absence of the hole, the structure resonates at 2025 MHz and after its introduction at 2035 MHz. With the introduction of an empty glass capillary (air inside), the resonance frequency is 2025 MHz, and on placing a glass capillary filled with water it shifts to 1960 MHz.

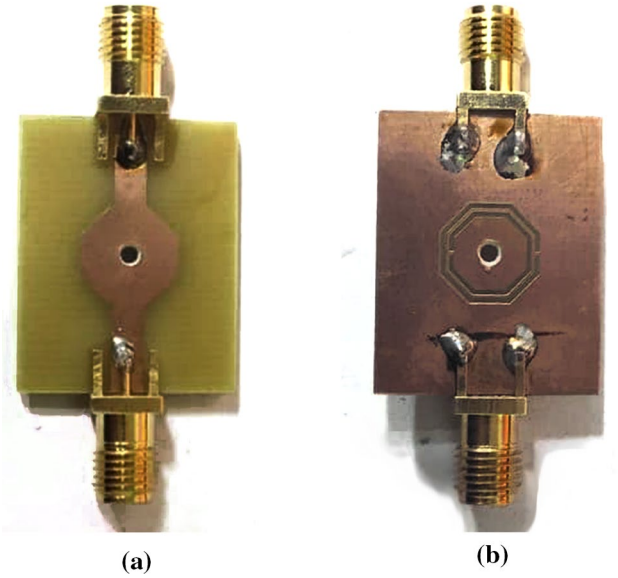

Fig. 4 Fabricated sensor prototype (a) top-view, and (b) bottom-view.

Measurement and Analysis

For investigating the relationship between complex permittivity (ε' and ε'') and f_o and Q factor, methanol-water and ethanol-water solutions were used. The concentration of water by volume in the solutions was varied with a step size of 10% and a transmission coefficient curve (S_{21}) was obtained. Since the CSRR has been designed to resonate near 2 GHz, the value of ε' and ε'' for methanol-water and ethanol-water solutions at 2 GHz are obtained from. Ref. 31.

The test-bench setup for the experiment is shown in Fig. 5. The fabricated prototype shown in Fig. 4 is connected to a vector network analyzer (VNA) (E5071C by Agilent Technologies). Sample solutions are drawn into a capillary and replaced for every reading. The experiment was conducted at room temperature and humidity which were recorded to be 27°C and 40%, respectively. To maintain the unbiased measurements, the solutions were labeled in codes and tested by a person unaware of the values. The person recorded the values of f_0 and Q for each sample from the S_{21} plot using the VNA and used the algorithm ("Appendix A") to obtain the values of ε' and ε''.

Study of Methanol–Water Solution

Figure 6 shows the variation of S_{21} with increase in concentration of water in solution. The curve shows a consistent increase in Q factor and the resonance frequency decreases from 1980 MHz at 0% water (pure methanol) to 1962 MHz at 100% water (pure water).

The varying concentration of water changes the permittivity of the solution, hence a relationship can be

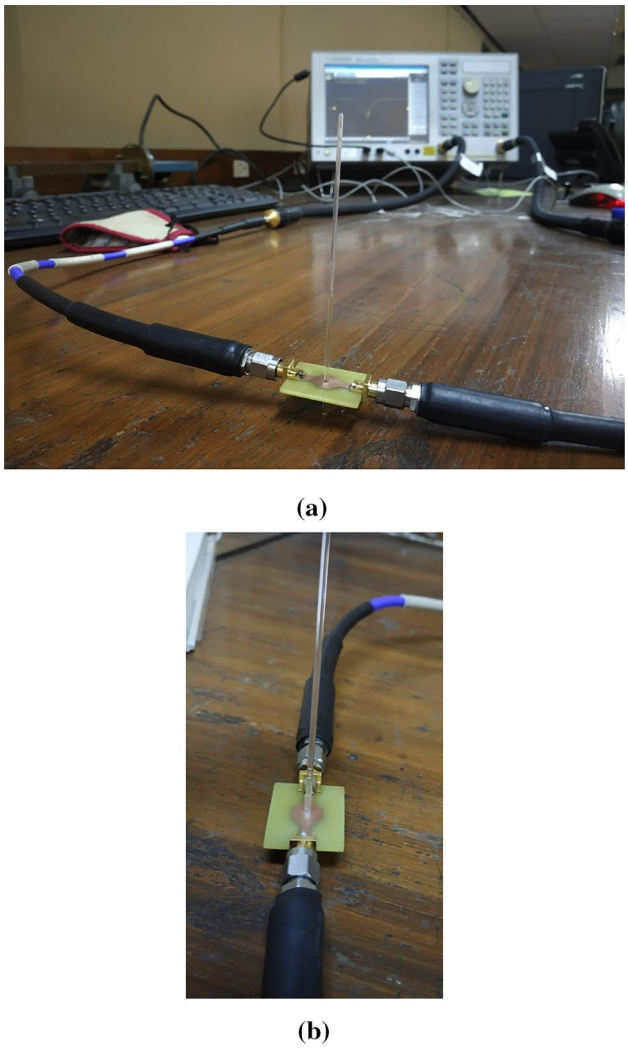

Fig. 5 (a) Test-bench setup for the testing of fabricated sensor using a vector network analyzer (VNA), and (b) Sensor prototype with sample fluid under test.

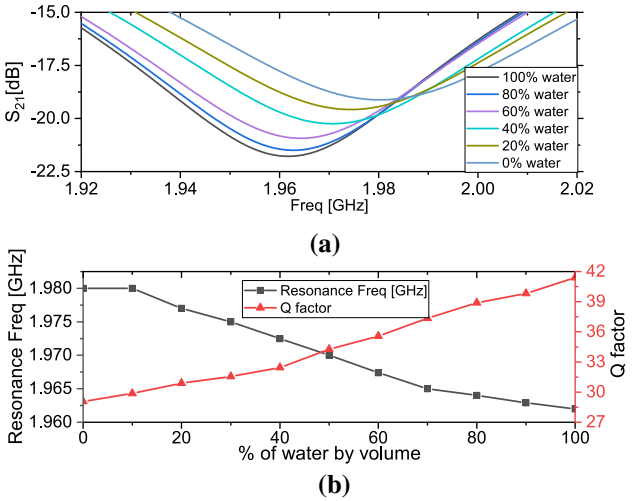

Fig. 6 (a) Variation in transmission coefficients (S_{21}) with a change in the concentration of water in the methanol-water solution and, (b) Corresponding resonance frequency (f_o) and Q factor plotted against the concentration of water with a step size of 10%. For visual clarity, only transmission coefficients (S_{21}) at intervals of 20% are shown.

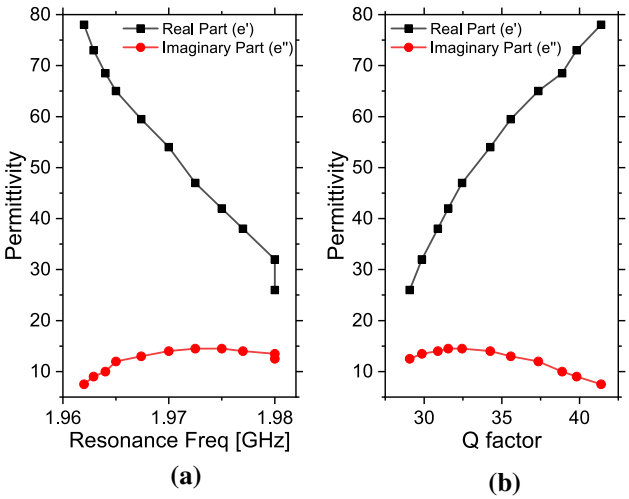

Fig. 7 Relationship between complex permittivity (ε' and ε'') with (a) resonance frequency (f_o) and, (b) Q factor for various concentration of water in methanol-water solution. A non-linear relationship can be observed in the plot.

established between the permittivity (ε' and ε''), resonance frequency and Q factor. Figure 7a shows a non-linear relationship between permittivity and f_o and Fig. 7b between permittivity and Q factor.

Since the curves in Fig. 7 show a non-linear relationship, a linear approximation as used by Refs. 7–10 results in a significant error during prediction. For proper curve fitting of ε' and ε'' with their dependence on f_o and Q multi-variate polynomial regression of second-order was used. We defined ε' and ε'' as functions of f_o and Q as f_1 and f_2 , respectively, in Eq. 5. The algorithm assumes f_1 and f_2 as second-order polynomials given by Eq. 6, where $a_0, a_1, ..a_5$ and $b_0, b_1, ..b_5$ are the constants to be estimated through the training data.

$$\begin{aligned} f_1 &= a_0 + a_1 f_o + a_2 Q + a_3 f_o^2 + a_4 f_o Q + a_5 Q^2, \\ f_2 &= b_0 + b_1 f_o + b_2 Q + b_3 f_o^2 + b_4 f_o Q + b_5 Q^2 \end{aligned} \tag{6}$$

The algorithm is trained on the 11 data points generated by varying water-methanol composition with a step size of 10% from 0% water to 100% water. The pseudo-code for the multi-variate polynomial regression used for the determination of constants and predicting the data is given in

Table I Values of constants Eq. 6 obtained for methanol-water solutions

a_0	$1.163 \times 10^{+06}$	b_0	$2.758 \times 10^{+05}$
a_1	$-1.142 \times 10^{+06}$	b_1	$-2.703 \times 10^{+05}$
a_2	$-2.161 \times 10^{+03}$	b_2	$-5.576 \times 10^{+02}$
a_3	$2.806 \times 10^{+05}$	b_3	$6.623 \times 10^{+04}$
a_4	$1.072 \times 10^{+03}$	b_4	$2.777 \times 10^{+02}$
a_5	7.718×10^{-01}	b_5	1.498×10^{-01}

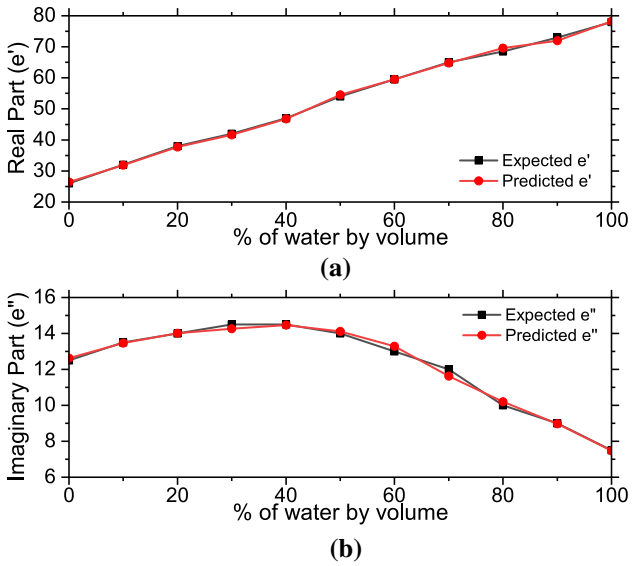

Fig. 8 Comparison between the expected values of complex permittivity (ε' and ε'') from Ref. 31 and the predicted values using multivariate polynomial regression of second-order for methanol-water solution.

"Appendix A". The values obtained for the constants are mentioned in Table I.

After estimating the values of constants in Eq. 6 the same equation can now be used to predict the values of ε' and ε'' for the methanol-water solution with an unknown concentration of water. The predicted values are plotted with the values of permittivity found by[31] as mentioned in Ref. 31 in Fig. 8.

The predicted values offer very low error as the predicted value is very close to the truth value. The results can be further improved by training the data on more points. Using a polynomial of third-order or higher requires the model to learn more coefficients which will require more data points to train. A second-order polynomial is appropriate for the given data as the error is greatly reduced as compared to the linear approximation in Refs. 7–10.

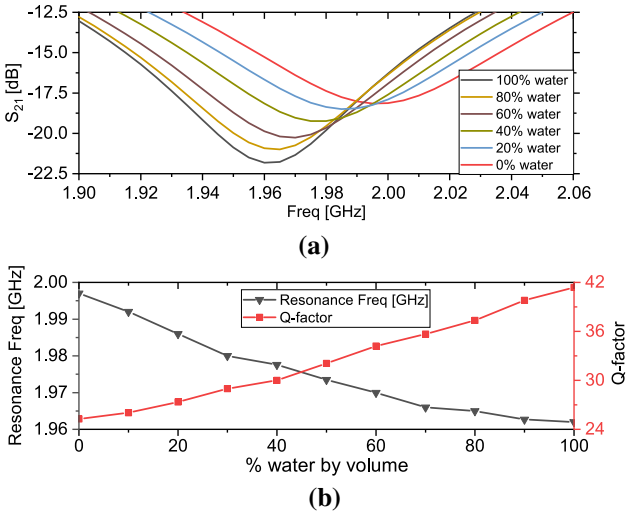

Fig. 9 (a) Variation in transmission coefficients (S_{21}) with change in concentration of water in ethanol-water solution and, (b) Corresponding resonance frequency (f_o) and Q factor plotted against concentration of water in the solution with step size of 10%. For visual clarity only transmission coefficients (S_{21}) at intervals of 20% are shown.

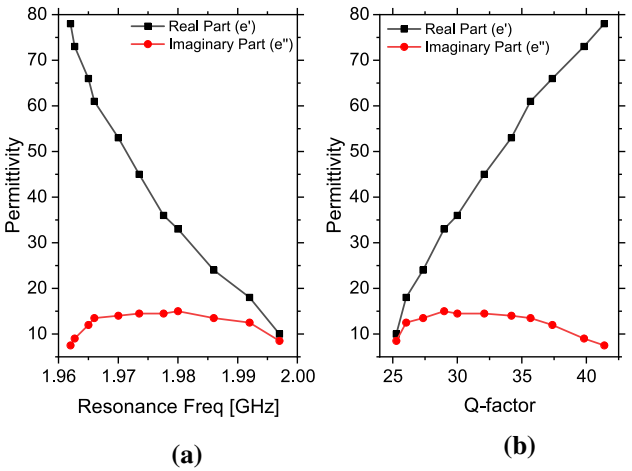

Fig. 10 Relationship between complex permittivity (ε' and ε'') with (a) resonance frequency (f_o) and, (b) Q factor for various concentration of water in ethanol-water solution. A non-linear relationship can be observed in the plot.

Study of Ethanol–Water Solution

A study similar to the methanol-water solution as shown in Sect. "Study of Methanol–Water Solution" is conducted for an ethanol-water solution as well. The step size for the concentration of water by volume is kept 10% this time as well. The transmission coefficient (S_{21}) curve follows the same trend for ethanol-water solution (Fig. 9) as it did for methanol-water solution (Fig. 6).

The variation of permittivity due to an increase in concentration of water in the ethanol-water solution and its

Table II Values of constants obtained for Eq. 6 for ethanol-water solutions

a_0	$-1.729 \times 10^{+05}$	b_0	$-1.544 \times 10^{+05}$
a_1	$1.692 \times 10^{+05}$	b_1	$1.520 \times 10^{+05}$
a_2	$4.326 \times 10^{+02}$	b_2	$2.848 \times 10^{+02}$
a_3	$-4.138 \times 10^{+04}$	b_3	$-3.741 \times 10^{+04}$
a_4	$-2.122 \times 10^{+02}$	b_4	$-1.392 \times 10^{+02}$
a_5	-1.802×10^{-01}	b_5	-1.641×10^{-01}

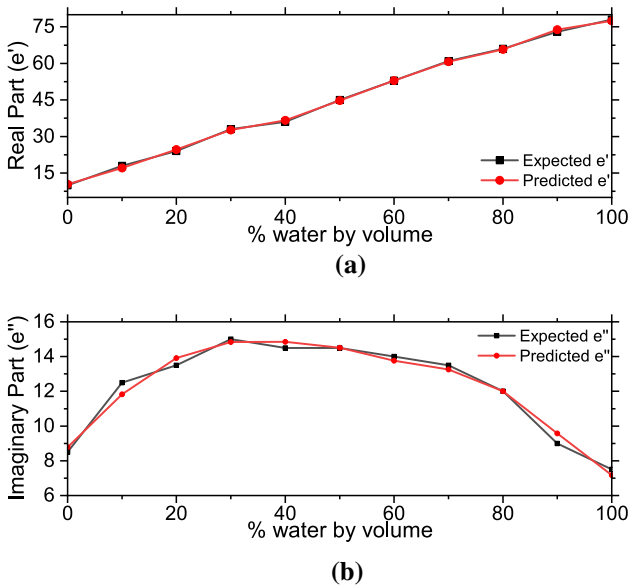

Fig. 11 Comparison between the expected values of complex permittivity (ε' and ε'') from [31] and the predicted values using multi-variate polynomial regression of second-order for ethanol-water solution.

affect on resonance frequency (f_o) and Q factor (Q) are demonstrated in Fig. 10. The non-linearity is similar to the curve obtained in the case of methanol-water solutions (refer to Fig. 7), and hence the second-order non-linear polynomial regression can be applied to achieve expressions for ε' and ε'' in terms of f_o and Q.

The constants for Eq. 6 are now estimated for the data points available from Fig. 10 and listed in Table II.

The estimated values obtained from the expression using the coefficients listed in Table II are plotted in Fig. 11. The estimated value using Eq. 6 is very close to the true value mentioned in Ref. 31.

The prediction of permittivity of solutions with such small errors indicates the benefit of using a higher-order approximation instead of a linear one. Another factor which affects the electric field and thus the transmission coefficient inside the fluid is its electrical conductivity (σ). For pure ethanol, conductivity is zero and for pure methanol and water, it is 44 $\mu S/cm$ and 200 $\mu S/cm$, respectively. Since the conductivity for the solutions is very low, its effect on the resonance frequency (f_o) and Q factor (Q) can be neglected. In the testing of samples with fluids of high electrical conductivity, the Eq. 5 will be modified to Eq. 7.

$$\begin{aligned} \varepsilon' &= f_1(f_o, Q, \sigma), \\ \varepsilon'' &= f_2(f_o, Q, \sigma) \end{aligned} \tag{7}$$

The pseudo-code in "Appendix A" can be modified to take three independent variables f_o, Q and σ as features to predict ε' and ε''. In the availability of more data points, the code can be used with even higher orders of polynomials at the cost of more computational time and memory.

Table III presents a brief performance comparison the work presented in this paper with earlier publish sensors for dielectric characterization. In Ref. 11 a very small sensor is proposed with dual band operation, increasing the complexity of analysis. In Ref. 14 the procedure for sample placement is not recommended as the sample under test is placed directly on the sensor surface which can cause damage to the sensor and may leave residue affecting the next sample. Similarly, in Refs. 9,16 a special container is designed for placement of the sensor which is not cost effective if a large number of samples are to be tested, and reusing the container may lead to inaccurate results due to residues. In Refs. 8,10,13 the sample fluid must be placed in a horizontal capillary, must be pumped through the container which increases the complexity of fabrication and analysis. The accuracy of prediction depends on the curve fitting method. The proposed sensors in Refs. 7, 8, 10, 13 use a linear first-order polynomial. In this paper, the authors propose a simple low-cost sensor with second-order polynomial curve fitting with easy to replace capillary for placement of sample under test.

Conclusion

A low-cost, simple and efficient CSRR based microwave sensor is introduced in this paper for dielectric characterization of fluids. The sensor operates near 2 GHz. The sample under test is placed in the vertical column and the complex permittivity of the sample fluid is estimated by the transmission coefficient curve. A relation between the resonance frequency (f_o) and Q factor (Q)) and (ε' and ε'') is established. The empirical relationship is modeled by a second-order polynomial and multi-variate polynomial regression is used to find the coefficients of the polynomial and then permittivity for solutions of unknown concentration of water is predicted using the obtained polynomial. The proposed sensor is fabricated and tested with methanol-water and ethanol water solutions. The predicted values of permittivity are in very good agreement with the truth value.

Table III Comparison of the proposed sensor with previously published sensors

Ref.	Sensor type	Resonant Frequency (GHz)	Size	Test Solution	Ease of Manufacture	Polynomial Fitting, Ease of Analysis	Sample Placement
Ref. 13	Circular CSRR	2.4	25 × 35	Water–ethanol	Complex	First-order, Simple	Horizontally Replaceable Capillary
Ref. 11	Circular CSRR	2.4, 5.8	12 × 20	Water–ethanol, Milk–urea	Simple	Third order, Complex	Vertically Replaceable pipette
Ref. 14	Modified CSRR	2.4	25 × 30	Food samples (liquids)	Simple	Second-order Complex	Sample placed directly on the sensor surface
Ref. 16	Labyrinth Resonator	4-5	>24 × 24	Water-ethanol, water–methanol	Moderate	– Complex to	Special container attached to a sensor
Ref. 9	Mu Negative Metamaterial (MNG)	1.5	4.8 × 4.8	Water–methanol	Moderate	Exponential, Complex	Polydimethylsiloxane (PDMS) well
Ref. 10	Square CSRR	2.4	20 × 28	Water–ethanol	Simple	First-order, Simple	Vertically Replaceable pipette
Ref. 8	Split Ring Resonator	1.9	28 × 30	Water–ethanol, water-methanol	Complex	First-order, Simple	Pumping of sample through horizontal capillary on sensor
Ref. 7	Split Ring Resonator	2.4	20 × 25	Water-ethanol	Complex	First-order, simple	Pumping of sample through PDMS channel
Prop.	Octogonal CSRR	2	20 × 25	Water–ethanol, water–methanol	Simple	Second order, Simple	Vertically Replaceable Capillary

Appendix A: Pseudo Code for Multi-Variate Polynomial Regression

1. Import Libraries [For python Pandas Numpy sklearn]
2. Read data from csv (comma separated values) file and convert it into a dataframe (say df)

   df = pandas . read_csv ("filename_with_extension")

   f = float (input (Enter the value of first input feature))

   Q = float (input (Enter the value of second input feature))

5. Generate polynomial and interaction features. The degree-2 polynomial features are [1, a, b, a^2, ab, b^2]. [Use PolynomialFeatures class from sklearn.preprocessing library for python]

   poly = sklearn.preprocessing.Polynomial Features (degree = DEGREE OF POLYNOMIAL YOU WANT TO CREATE)

   poly_variables = poly.fit_transform(arrayofvaluesofinputfeatures)

3. There are 2 training data columns of 2 target columns to be predicted. Extract only required columns from dataframe.

   train _features = [’column1’, ’column2’]

   target_column_1 = df [’target1’]

   target_column_2 = df [’target2’]

   data = df [’train_features’]

4. Take the input of two train_features values (f and Q) to predict target values (ε' and ε'')

6. Repeat the above process for test values for which we are predicting output values:

   test_variables = poly.fit_transform (an array of input values f and Q)

7. To create model, use simple linear regression. [Use LinearRegression from library sklearn.linear_model for python]

   regression = sklearn.linear_model.LinearRegression ( )

   model = regression.fit(poly_variables,target_column_1)

8. Obtain the coefficients and intercept of fitted equation.

   print(coefficients of fitted/learned equation)
   print(intercept of fitted/learned equation)

9. Predict the model. [Use model.predict() for python]

   prediction = model.predict(test_variables)
   print(prediction)

10. Repeat 7, 8 and 9 for second target column to predict another target value. We have to use 2 separate models for training, as it is multi-target regression problem.

Acknowledgments All authors certify that they have no affiliations with or involvement in any organization or entity with any financial interest or non-financial interest in the subject matter or materials discussed in this manuscript.

Data Availability The data that support the findings of this study are openly available in GitHub at https://github.com/msingh189/Fiiting_polynomial_surface.

Conflict of interest The authors have no conflicts of interest to declare that are relevant to the content of this article.

References

1. R. Joffe, E.O. Kamenetskii, R. Shavit, *J. Appl. Phys.* 1130(6), 0063912 (2013)
2. J. Bourqui, E.C. Fear, Shielded uwb sensor for biomedical applications. *IEEE Antennas Wirel. Propag. Lett.* 11, 1614 (2012)
3. J. H. Goh, A. Mason, A. I. Al-Shamma'a, S. R. Wylie, M. Field, P. Browning. Lactate detection using a microwave cavity sensor for biomedical applications. In 2011 Fifth International Conference on Sensing Technology, pages 436–441, 2011.
4. M. Birkholz, K.-E. Ehwald, T. Basmer, P. Kulse, C. Reich, J. Drews, D. Genschow, U. Haak, S. Marschmeyer, E. Matthus, K. Schulz, D. Wolansky, W. Winkler, T. Guschauski, R. Ehwald, *J. Appl. Phys.* 1130(24), 244904 (2013)
5. C. Jang, J. Park, H. Lee, G. Yun, J. Yook, *IEEE Sens. J.* 200(15), 8520– (2020). https://doi.org/10.1109/JSEN.2020.2984779
6. A.J. Cole, P.R. Young, *IEEE Sens. J.* 180(1), 149 (2018)
7. A. Ebrahimi, W. Withayachumnankul, S. Al-Sarawi, D. Abbott, *IEEE Sens. J.* 140(5), 1345 (2014)
8. W. Withayachumnankul, K. Jaruwongrungsee, A. Tuantranont, C. Fumeaux, D. Abbott, *Sens. Actuators A Phys.* 189, 233 (2013)
9. S. Kayal, T. Shaw, D. Mitra, *Appl. Phys. A* 1260(1), 13 (2019)
10. E.L. Chuma, Y. Iano, G. Fontgalland, L.L. Bravo Roger, *IEEE Sens. J.* 180(24), 9978 (2018)
11. K.Y. Yogita, K. Awasthi, *J. Electr. Mater.* 490(1), 385 (2020)
12. M.A. Tümkaya, F. Dinçer, M. Karaaslan, C. Sabah, *J. Electr. Mater.* 460(8), 4955 (2017)
13. E.L. Chuma, Y. Iano, G. Fontgalland, L.L.B. Roger, H. Loschi, *Sens. Actuators A Phys.* 312, 112112 (2020)
14. X. Zhang, C. Ruan, K. Chen, *Sensors* (2019). https://doi.org/10.3390/s19040787
15. X. Bao, I. Ocket, J. Bao, Z. Liu, B. Puers, D.M.M. Schreurs, B. Nauwelaers, *IEEE Trans. Microw. Theory Tech.* 670(7), 2674 (2019). https://doi.org/10.1109/TMTT.2019.2916871
16. O. Altintaş, M. Aksoy, E. Ünal, M. Karaaslan, *J. Electrochem. Soc.* 1660(6), B482 (2019)
17. O. Altıntaş, M. Aksoy, E. Ünal, *Phys. E Low-Dimens. Syst. Nanostruct.* 116, 113734 (2020)
18. S. Trabelsi, S.O. Nelson, *IEEE Instrum. Measurement Mag.* 190(1), 36 (2016)
19. M.S. Venkatesh, G.S.V. Raghavan, *Biosyst. Eng.* 880(1), 1 (2004)
20. M.F. Mabrook, M.C. Petty, *Sens. Actuators B Chem.* 960(1), 215 (2003)
21. M.H. Zarifi, A. Sohrabi, P.M. Shaibani, M. Daneshmand, T. Thundat, *IEEE Sens. J.* 150(1), 248 (2015)
22. R. Melik, E. Unal, N.K. Perkgoz, C. Puttlitz, H.V. Demir, *Appl. Phys. Lett.* 950(1), 011106 (2009)
23. C. Mandel, M. Schüßler, R. Jakoby, *SENSORS* (2011). https://doi.org/10.1109/ICSENS.2011.6126942
24. C. Mandel, B. Kubina, M. Schüßler, R. Jakoby. Passive chipless wireless sensor for two-dimensional displacement measurement. In 2011 41st European Microwave Conference, pages 79–82. https://doi.org/10.23919/EuMC.2011.6101801. (2011).
25. Z. Zhang, X. Liao, *IEEE Sens. J.* 150(4), 2019 (2015). https://doi.org/10.1109/JSEN.2014.2382719
26. K. Lee, J. Kim, C. Cha. Microwave-based wireless power transfer using beam scanning for wireless sensors. In IEEE EUROCON 2019 -18th International Conference on Smart Technologies, pages 1–5, 2019. 10.1109/EUROCON.2019.8861838.
27. M. D'Asaro, D. Sheen, J. Lang. A fully-shielded flexible and stretchable microwave transmission-line tactile pressure sensor. In 2016 IEEE SENSORS, pages 1–3, 2016. 10.1109/ICSENS.2016.7808912.
28. H. Nakano. Categorization of Natural Materials and Metamaterials, pages 1–10. (2016).
29. R. k. Baee, G. Dadashzadeh, F. G. Kharakhili. Using of csrr and its equivalent circuit model in size reduction of microstrip antenna. In 2007 Asia-Pacific Microwave Conference, pages 1–4, (2007).
30. J. Bonache, M. Gil, I. Gil, J. Garcia-Garcia, F. Martin, *IEEE Microwave Wirel. Compon. Lett.* 160(10), 543 (2006)
31. J.-Z. Bao, M.L. Swicord, C.C. Davis, *J. Chem. Phys.* 1040(12), 4441 (1996)